AN ELECTROCHEMICAL IMPEDANCE SPECTROSCOPY STUDY OF HYDRAZINE OXIDATION ON Pd SUPPORTED ON GRAPHITE CLOTH

Duarte*, M.M.E.; Stefenel, M.M.; Mayer, C.E.

Instituto de Ingeniería Electroquímica y Corrosión – INIEC; Departamento de Ingeniería Química. Universidad Nacional del Sur. Av. Alem 1253.8000 Bahía Blanca. Argentina.
e-mail: mduarte@criba.edu.ar

Received March 27, 2000. In final form: October 17, 2002

Abstract

The electro-oxidation of hydrazine in alkaline media on palladium dispersed over electrochemically modified graphite cloth is studied using EIS measurements. The impedance behavior is rather complex since it includes effects that arise from electrode structure, interfacial graphite properties and reaction kinetics. A small and distorted semicircle appears in the high frequency region that is attributed to the porous structure of the electrode. The existence of an adsorbed intermediate was detected at very low currents. A low frequency loop was observed in the high current range that arises from the development of concentration gradients inside the pores.

Resumen

Se estudia la electrooxidación de hidracina sobre paladio dispersado sobre telas de grafito modificadas electroquímicamente, en medio alcalino, utilizando espectroscopía de impedancia electroquímica. La impedancia del sistema es bastante compleja, dado que es consecuencia de la estructura del electrodo, las propiedades interfaciales del grafito y la cinética de la reacción. Un pequeño semicírculo deformado aparece en la región de altas frecuencias, el que se atribuye a la estructura porosa del electrodo. A corrientes bajas se detecta la existencia de un intermediario adsorbido. En el rango de altas corrientes, a bajas frecuencias, se observa un semicírculo que se debe al desarrollo de gradientes de concentración en el interior de los poros.

Introduction

Commercial carbon fiber cloths and felts constitute a particular type of porous electrode, being attractive material for using as catalyst substrate in anodes for liquid organic fuels in low temperature fuel cells [1].

It is known that the heterogeneous electron transfer reactions at graphite, glassy carbon, etc., are sensitive to the microscopic structure of the surface, particularly the nature and density of carbon-oxygen functional groups. Hence, considerable effort has been devoted to developing electrode pre-treatments that give reproducible results.

Recently, the behavior of graphite fiber electrodes modified by electro-oxidative pre-treatments in sulfuric acid solution at potentials between 1.9 and 2.4 V was studied [2, 3]. The first changes occur on the surface, with an increase of surface roughness and electrode activation by a higher concentration of surface oxides. After long treatment times, the electrode becomes passive by formation of a multilayer oxide which inhibits characteristic electrochemical processes.

In most cases, graphite fibers must be electrochemically oxidized as first step in the incorporation of the catalyst, which is generally a platinum group metal. For example, palladium catalyzed fibers are very suitable materials for the hydrogen evolution reaction, presenting a strong catalytic activity, which is due to the high dispersion of palladium on the carbon support.

Graphite cloth electrodes performance can be evaluated through polarization curves that permit to compare the effect of electrode structure, catalyst surface area, electrocatalytic activity and other characteristic parameters. However, interpretation of results is ambiguous in many cases and it is difficult to separate the different contributions to electrode behavior.

Electrochemical impedance spectroscopy (EIS) is a technique that allows us to evaluate the comparative importance of different factors. It has been applied to porous electrode systems such as gas diffusion electrodes [4, 5], batteries [6], formic acid porous electrodes [7] and fuel cells [8].

Hydrazine is one of the most attractive fuels used in fuel cells with alkaline electrolyte. Three properties are mainly responsible for this position: high energy density in relation to volume and weight; good electrochemical activity under anodic oxidation and reaction products that do not contaminate the electrolyte [9].

In this work the electro-oxidation of hydrazine in alkaline media on palladium dispersed over electrochemically modified graphite cloth, is studied using EIS measurements.

Experimental

The electrodes were made of graphite fiber cloth (The Electrosynthesis Company, Inc.) catalyzed with palladium. The method of preparation consisted of an initial potentiostatic oxidation at 2.0 V (ENH) in 0.5 M H_2SO_4 for a given time, followed by a cathodic sweep at 0.01 $V.s^{-1}$ in order to reduce the oxide formed in these conditions [10]. Afterward the electrode was immersed three hours in distilled water, dried superficially and impregnated with 0.23 M $PdCl_2$ solution. Results are reported for two electrodes – named A and B- both prepared under similar conditions, differing only in the extent of the oxidative treatment. Most results were obtained with electrode A, which was oxidized for 2 minutes, while electrode B was subject to intensive oxidation for 60 minutes. Palladium surface area was determined by cyclic voltammetry [11] using the charge of the palladium oxide peak in 0.5 M H_2SO_4. Relative surface areas of 150 and 400 cm^2 per cm^2 geometric area were measured for electrodes A and B respectively.

For EIS measurements, a conventional glass cell was used. A platinized Pt sheet was used as the counter-electrode. A saturated calomel electrode with a Haber-Luggin capillary tip served as the reference electrode, although all potentials are referred to the

normal hydrogen electrode. All solutions were prepared from p.a. reagents and distilled water. Impedance measurements were carried out in 25 % KOH + 3 % N_2H_4 and 5 % KOH + 0.6 % N_2H_4, at room temperature.

The impedance spectra were obtained in the frequency range $0.01 < f < 10000$ Hz. Galvanostatic control was used, and the equipment consisted of a Solartron FRA 1250 frequency analyzer integrated with a Solartron 1286 electrochemical interface and a personal computer. A platinum probe was connected to the reference electrode through a capacitor to reduce phase error at high frequencies.

Results and discussion

Steady state current density - potential curves were obtained for both electrodes at two different concentrations of N_2H_4 (Figure 1). The points correspond to the current densities at which impedance measurements were made. For electrode A, both set of measurements exhibit similar Tafel slopes in the range of low current densities. The values of the stationary slopes are about 0.04 V for 3 % N_2H_4 and 0.03 V for 0.6 %. At higher currents the Tafel slope increases due to the existence of concentration gradients [12]. Electrode B, which was object of strong oxidation, exhibited higher catalytic activity and the current - potential curves showed a slope of 0.025 V independent of the concentration.

The electrochemical oxidation of hydrazine in alkaline media has a mixed rest potential generally accepted to be determined by the anodic oxidation of N_2H_4 [13]

$$N_2H_4 + 4\ OH^- \rightarrow N_2 + 4\ H_2O + 4\ e^- \qquad E^0 = -1.16\ V \qquad [I]$$

and one of the following cathodic reduction reactions:

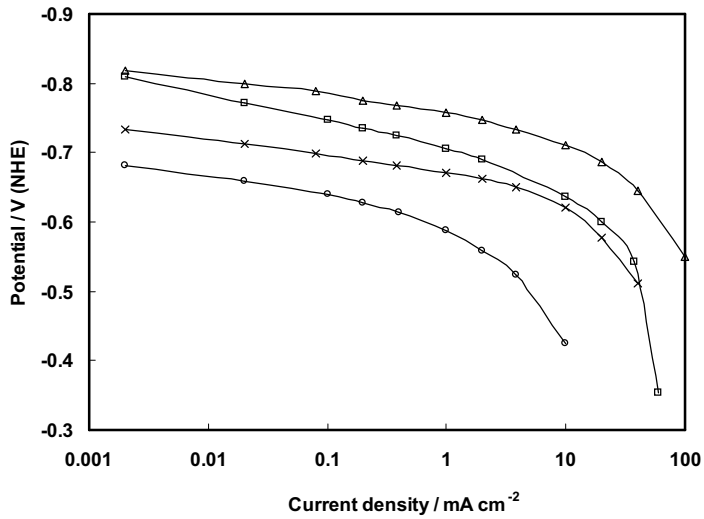

Figure 1: *Steady-state current density - potential curves for anodic hydrazine oxidation on electrode A, C_{N2H4}= 3 % (□); C_{N2H4}= 0.6 % (O), and electrode B, C_{N2H4}= 3 % (Δ); C_{N2H4}= 0.6 % (X).*

$$2\ H_2O + 2\ e^- \rightarrow H_2 + 2\ OH^- \qquad E^0 = -0.826\ V \qquad [II]$$

$$N_2H_4 + 4\ H_2O + 2\ e^- \rightarrow 2\ NH_4OH + 2\ OH^- \qquad E^0 = 0.080\ V \qquad [III]$$

Only reaction [II] is thought to occur at an appreciable rate at the mixed rest potential, especially at low concentration of N_2H_4, whereas reaction [III] is more pronounced on platinized carbon electrode.

For oxidation of N_2H_4 on palladium electrodes a mechanism based on the formation of adsorbed intermediates has been proposed [14, 15], following the reaction scheme

$$N_2H_4\,(ad) + OH^- \rightarrow N_2H_3\,(ad) + H_2O + e^- \qquad [IV]$$

$$N_2H_3\,(ad) \rightarrow N_2 + 3\ H\,(ad) \qquad [V]$$

$$H\,(ad) + OH^- \rightarrow H_2O + e^- \qquad [VI]$$

It is generally admitted that reaction [VI] is the rate-determining step while reaction [IV] and [V] are assumed to be almost in equilibrium. As a consequence, hydrogen accumulation on the metal surface and in the bulk may be expected.

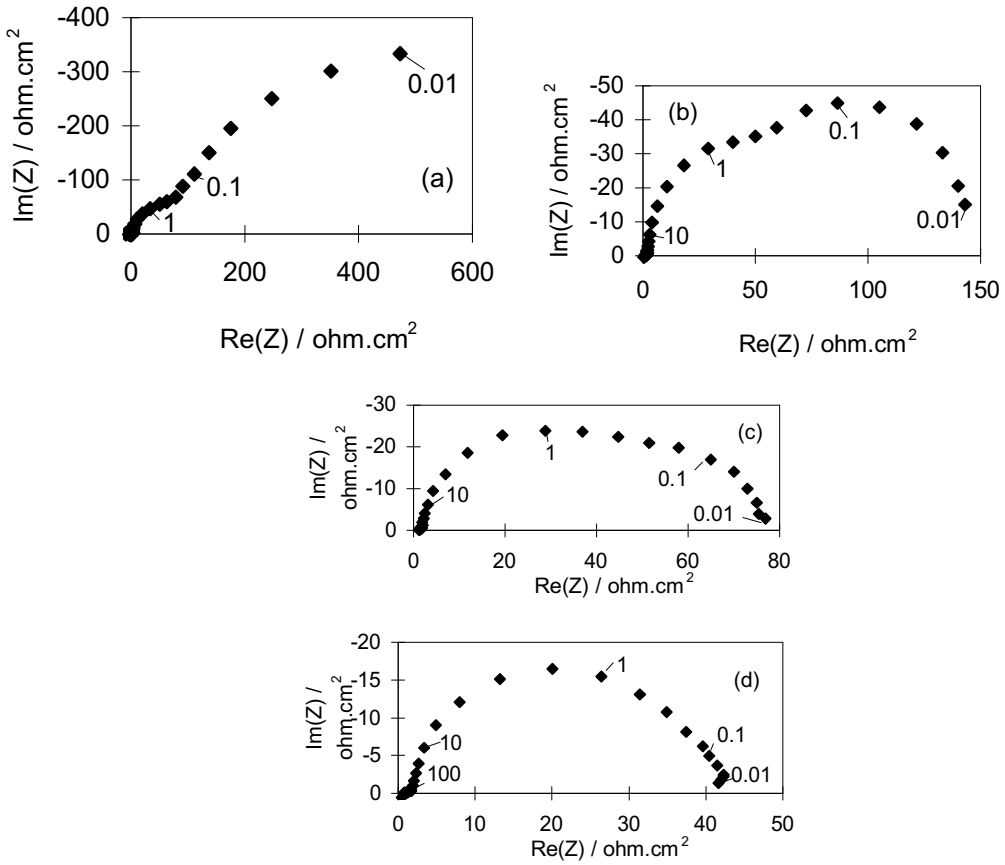

Figure 2: *Impedance spectra for anodic hydrazine oxidation in the low current density range. Electrode A: C_{N2H4}= 3 %, current density = 0.02 mA.cm^{-2} (a), 0.1 mA.cm^{-2} (b), 0.2 mA.cm^{-2} (c), 0.4 mA.cm^{-2} (d). C_{N2H4}= 0.6 %.*

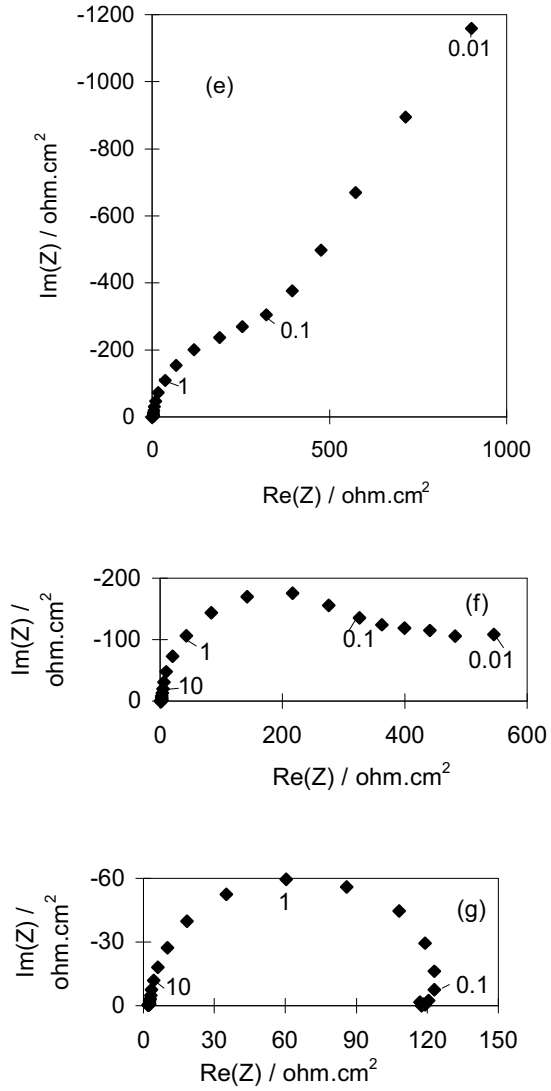

Figure 2: Cont. *Impedance spectra for anodic hydrazine oxidation in the low current density range. Current density = 0.002 mA.cm^{-2} (e), 0.02 mA.cm^{-2} (f), 0.1 mA.cm^{-2} (g).*

In this work, rest potentials between -0.825 and -0.850 V have been measured for the higher concentration. This value is approximated to the equilibrium potential of reaction [II] and is consistent with the reaction scheme given above.

Figure 2 shows the complex plane impedance diagrams for the lower currents densities. The points represent the experimental data. In the usual way, the numbers give the frequencies in Hz. The impedance spectra obtained in the low current density range consists of following elements:

a) A small distorted semicircle in the high frequency region (HF) that at low currents is masked by the medium frequency loop (Figure 2d).

b) A medium frequency capacitive arc (MF).

c) A low frequency capacitive semicircle (LF), that depends strongly on the current. Its diameter decreases with increasing anodic polarization until it merges with the medium

frequency semicircle into a single highly distorted loop, which gradually approaches an ideal semicircle (Figure 3a). This behavior is characteristics of a reaction mechanism with adsorbed intermediates, in which diffusion of participating species is not rate limiting [16]. Under certain conditions the LF arc shows the behavior of an inductance. Comparing (b) and (g) in Figure 2, an inductive- to-capacitive transition in the impedance spectra is observed for different concentrations, which may arise from a change in the kinetics of N_2H_4 oxidation.

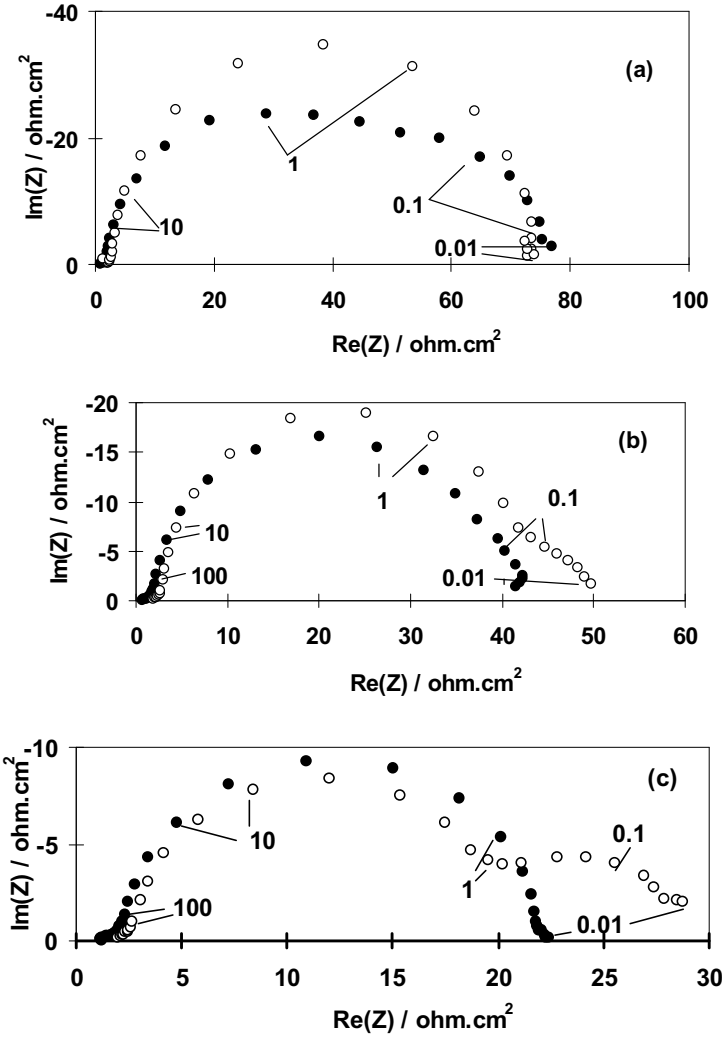

Figure 3: *Impedance spectra for anodic hydrazine oxidation showing concentration effect. Electrode A: C_{N2H4}= 3 % (●), C_{N2H4}= 0.6 % (O), current density = 0.2 mA.cm^{-2} (a), 0.4 mA.cm^{-2} (b), 1 mA.cm^{-2} (c).*

Another characteristic of the complex impedance of this system becomes apparent in Figure 3. When hydrazine concentration is low a single loop is observed at 0.2 mA.cm^{-2}, but at 0.4 mA.cm^{-2} a new loop begins developing in the low frequency range. For higher concentrations it is visible as point dispersion in the low frequency limit. Its appearance happens simultaneously with the change in the slope of the steady-state

current - potential curves (Figure 1). Porous electrode theory predicts the appearance of diffusion loops in the low frequency range [17, 18], originating in the concentration gradients arising in the pores. However it is also possible the existence of another process associated to the same reaction, which would be rate determining under the indicated conditions.

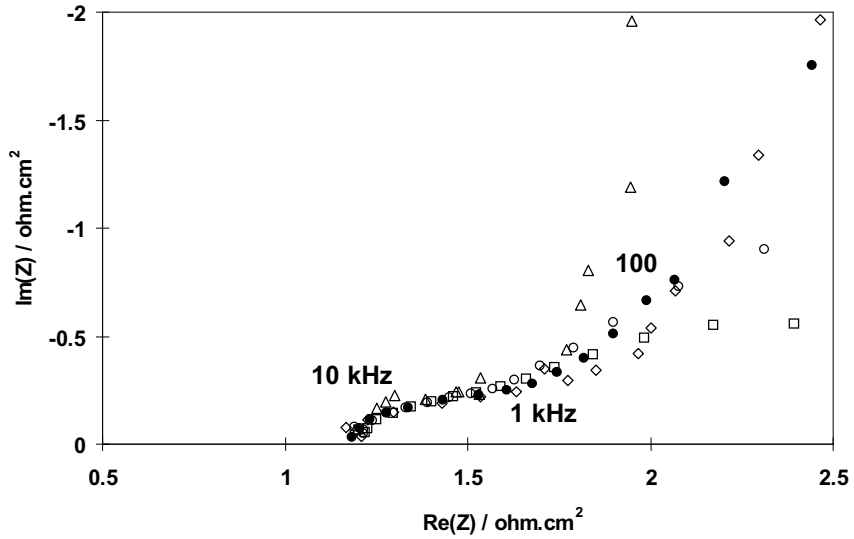

Figure 4: *Impedance spectra for anodic hydrazine oxidation showing the high frequency semicircle. Electrode A: C_{N2H4}= 3 %,,current density = 0.2 mA.cm^{-2} (Δ), 1 mA.cm^{-2} (◊), 2 mA.cm^{-2} (●), 10 mA.cm^{-2} (O), 20 mA.cm^{-2} (□).*

Figure 4 shows the HF semicircle for several current densities. Its size remains almost unchanged for different current densities showing a slight dependence on concentration. It is postulated that it is linked to the porous structure of the electrode. Such a phenomenon has already been observed [19, 20], and it is connected with the porosity of the electrode structure and not with any faradaic process. This effect arises from the alternate signal lagging in the inner surface of the pores. As a consequence the electrode behaves at high frequencies as if its surface area was lower. The penetration depth increases when the frequency decreases [17, 18, 21]. A straight line of unit slope, at high frequencies, is predicted for porous electrode theory for a cylindrical pore and infinite conductivity of the electrolyte [20]. In this particular case, no straight line is observed. This behavior probably arises from the particular cloth structure where two widely different pore sizes exist. The larger pores are the spaces between the threads and the smaller pores are defined by the space between the individual fibers, being the surface area of the larger pores more accessible. It may be expected that the smaller pores generate signal dispersion in a wider frequency range than the larger ones, leading to the observed behavior. The semicircle concentration dependence can be understood as being the result of pore blocking presumably by bubbles due to the intense nitrogen evolution at high potentials.

An increase of the impedance was observed at low frequency under conditions of high currents and low concentrations. This behavior may correspond to the onset of

Warburg impedance, and it may arise from limitations of mass transfer from bulk electrolyte to the external face of the electrode. However it has not been possible extend the frequency range to obtain a better definition, due to noises originating in bubble evolution and the difficulty in attaining the steady state for long times.

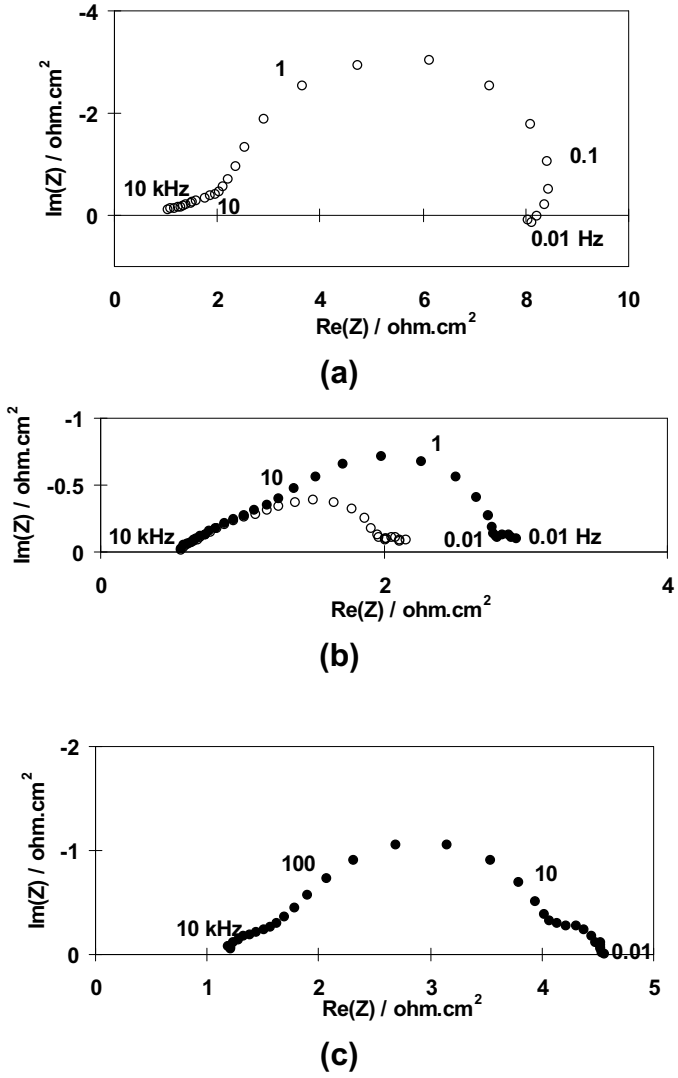

Figure 5: *Impedance spectra for electrode B, a) C_{N2H4}= 0.6%, 2 mA.cm^{-2}. b) C_{N2H4}= 3% (●) 10 mA.cm^{-2}, (O) 20 mA.cm^{-2}. c) Electrode A, C_{N2H4}= 3%, 10 mA.cm^{-2}.*

Results for electrode B, which was subject to more extensive oxidation, are shown in Figure 5. The inductive contribution to the electrode impedance cited previously can be distinguished for this electrode at intermediate currents (Figure 5a). The Nyquist diagrams for high current densities are shown in Figure 5b, being compared with the response in similar conditions of the electrode A (Figure 5c). In the impedance spectra, the HF loop appears superimposed to the MF semicircle while the LF loop is clearly separated. The impedance profiles shown in Figures 2 to 5 can be described by

transfer functions, corresponding to the equivalent circuit of Figure 6, which was selected using the EQUIVCRT program [23, 24]. The optimum numerical values of the equivalent circuit parameters are listed in Tables 1 and 2. Constant phase elements (CPE) [25] must be introduced in the equivalent circuit to account for frequency dispersion originating from heterogeneity or roughness of the electrode surface. The double layer capacitance should then be substituted by the constant phase element whose impedance may be described as:

$$Z_{CPE} = 1/[C(j\omega)^n] \quad (1)$$

where C is a real frequency-independent parameter related to the double layer capacitance, with units of $F.cm^{-2}.s^{n-1}$, and the exponent n is a constant ($-1<n<1$). When n = 1, a purely capacitive behavior is observed, whereas when n = 0 the CPE is considered to be a resistor.

In the following discussion distinction is made between the constant phase elements CPE_2 and CPE_3 to account for the differences observed in the LF half-circle at low and high current densities (see Figures 2 to 4).

The ohmic resistance of the electrolyte is in series with the parallel circuit that gives origin to the HF loop, which components are CPE_p and R_p. Table 1 shows the values of high frequency half-circle elements. As can be seen, the value of the exponent n_p oscillates around 0.5 for both electrodes.

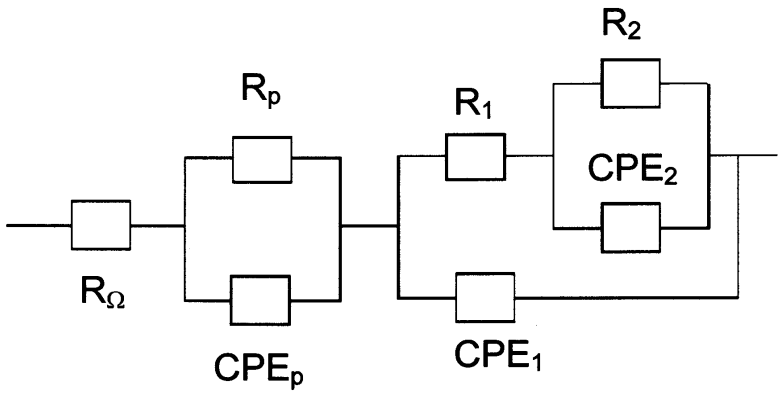

Figure 6: *Equivalent electrical circuit used for analysis of the impedance data.*

The other part of the circuit is characteristic of a reaction mechanism with adsorbed intermediates, in which diffusion of participating species is not rate limiting [16]. We associate the medium frequency semicircle element CPE_1 with the double layer capacitance. It is possible that adsorption of the intermediate might alter the charge of the double-layer (additionally to the faradaic contribution). However we assume that this effect is small. As can be seen in Table 2, C_1 for electrode A remains relatively constant for each concentration, although a slight decreasing is observed at high currents in some cases. This effect may be originated by a reduced penetration depth or by a decrease of the active surface area by nitrogen bubbles. The measured values are rather high, as should be expected, since both graphite fiber substrate and catalyst contributions are included.

i ($mA.cm^{-2}$)	C_{N2H4} (%)	R_{ohm} ($\Omega.cm^2$)	R_p ($\Omega.cm^2$)	$C_p \times 10^6$ ($F.cm^{-2}.s^{n-1}$)	n_p	C_1 ($F.cm^{-2}.s^{n-1}$)	n_1
0.2	3	1.1	0.67	4.05×10^{-4}	0.64	3.04×10^{-3}	0.93
0.38		1.1	1.16	1.68×10^{-3}	0.52	2.4×10^{-3}	1.0
1		1.18	1.12	6.97×10^{-4}	0.55	2.55×10^{-3}	0.96
2		1.14	0.89	3.02×10^{-4}	0.65	2.75×10^{-3}	0.95
10		1.08	0.91	1.33×10^{-3}	0.49	3.08×10^{-3}	0.95
0.2	0.6	0.93	1.28	2.93×10^{-2}	0.5	6.28×10^{-2}	0.91
0.38		0.81	1.61	5.68×10^{-2}	0.39	6.06×10^{-2}	0.94
1		0.92	1.76	6.19×10^{-2}	0.38	5.59×10^{-2}	0.96
2		0.89	1.93	7.09×10^{-2}	0.36	5.59×10^{-2}	0.99
20		0.90	1.68	9.94×10^{-2}	0.35	7.91×10^{-2}	1.00
2*	3	0.57	1.09	6.5×10^{-2}	0.5	7.46×10^{-2}	0.99
10*		0.55	1.29	7.98×10^{-2}	0.46	6.44×10^{-2}	1.00
20*		0.56	1.08	6.50×10^{-2}	0.5	7.6×10^{-2}	0.99

Table 1. *Elements of the high frequency loop. * Results for electrode B*

i $mAcm^{-2}$	c_{N2H4} (%)	CPE_1		R_1	CPE_2		R_2	CPE_3		R_3
		$C_1 \times 10^6$ ($F.cm^{-2}s^{n-1}$)	n_1	($\Omega.cm^2$)	C_2 ($F.cm^{-2}s^{n-1}$)	n_2	($\Omega.cm^2$)	C_3 ($F.cm^{-2}s^{n-1}$)	n_3	($\Omega.cm^2$)
0.1	3	2700	0.97	63.5	0.02118	0.89	82			
0.2		3040	0.93	53.3	0.05034	0.97	21.4			
0.38		2400	1.00	26.8	0.0277	0.58	14.9			
1		2550	0.96	19.7						
2		2750	0.95	10.6						
10		3080	0.95	2.14				0.6794	0.91	0.43
20		2710	0.95	0.95				0.6074	0.74	0.44
0.02	0.6	1540	0.95	842						
0.2		1460	0.98	141						
1		1420	0.99	33.4				0.1112	0.84	9.3
2		1350	0.97	19.8				0.1258	0.87	4.405
3.8		1200	0.97	9.3				0.185	1.00	0.92
0.2*	0.6	62800	0.91	90.5						
0.38*		60600	0.94	51.6						
1*		55900	0.96	20.7						
2*		55900	0.99	10.5						
2*	3	74600	0.99	0.92				39.6	0.87	0.179
10*		64400	1.00	2.11				12.22	1.00	0.11

Table 2. *Elements of the equivalent circuits. * Results for electrode B*

On the other hand, C_1 values for electrode B are more than one order of magnitude higher than for electrode A. The differences in palladium surface area are not sufficient to justify this variation. Therefore, the high capacitance must arise from the oxidized graphite substrate, since the principal difference between both electrodes is the oxidation time in the pre-treatment step [26]. The charge-transfer resistance R_1,

associated to the MF capacitive half-circle, decreases with increasing polarization and depends on the concentration and on the electrode properties.

The second capacitance C_2 is exceptionally high, even for a porous electrode, and at low currents it may be associated to an adsorption pseudo-capacitance. In these conditions, the resistance R_2 is associated with relaxation of coverage [16]. Considering the reaction scheme given by reaction [IV] to [VI], the adsorption capacitance C_2 may be associated to the H(ad) species.

The circuit component designed as CPE_3 is associated to a process that is important at high current densities, probably a diffusion step as mentioned above.

Conclusions

The steady state current density – potential curves and the experimental impedance data indicates the higher catalytic activity of the graphite fiber cloths electrode, which was object of strong oxidation pre-treatment. The impedance data confirms that the mechanism of the anodic oxidation of hydrazine on palladium loaded over graphite cloths electrodes may proceed through the formation of intermediate radicals, which readily decompose into hydrogen and relate compounds. The exceptionally high adsorption capacitance C_2 may be associated to the H(ad) species.

Acknowledgements

The authors acknowledge financial support from the Universidad Nacional del Sur, from the Comisión de Investigaciones Científicas de la Provincia de Buenos Aires (CIC) / Argentina and the Volkswagen Foundation / Germany. D.M.M.E. and M.C.E. are members of the CIC.

References

[1] Attwood,P.A.; McNicol, B.D.; Short, R.T. *J. Appl. Electrochem*. **1980**, *10*, 213.
[2] Duarte, M.M.; Mayer, C.E. *An. Asoc. Quím. Argent.* **1997**, *85*, 27.
[3] Andonoglou, Ph.P.; Jannakoudakis, A.D. *Electrochim. Acta*, **1997**, *42*, 1905.
[4] Wabner, D.; Holze, R.; Schmittinger, P. *Z. Naturforschung*. **1984**, *39b*, 157.
[5] Holze, R.;Vielstich, W. *Electrochim. Acta* **1984**, *29*, 607.
[6] Hampson, N.A.; Karunathilaka, S.A.G.; Leek, R. *J. Appl. Electrochem*. **1980**, *10*, 3.
[7] Holze, R.; Castro Luna, A.M. *J. Appl. Electrochem.* **1988**, *18*, 679.
[8] Jenseit, W.; Böhme, O.; Leidlich, F.U.; Wendt, H. *Electrochim. Acta* **1993**, *38*, 2115.
[1] [9] Gutjahr, M.A. In *From Electrocatalysis to Fuel Cells* (Sandstede, G. Ed.) University of Washington Press, **1972**, p.143.
[10] Duarte, M.M.E; Pilla, A.S.; Mayer, C.E. *An. Asoc. Quim. Argent.* **1993**, *81*, 415.
[11] Duarte, M.M.E.; Taberner, P.M.; Mayer, C.E. *Electrochim. Acta* 1989, **34**, 499.
[12] Austin, L.G. *Trans. Farad. Soc*. **1964**, *60*, 1319.
[13] Kodera, T.; Honda, M.; Kita, H. *Electrochim. Acta* **1985**, *30*, 669.
[14] Korovin, N.V.; Yanchuk, B.N. *Electrochim.Acta* **1970**, *15*, 569.
[15] Fukumoto, Y.; Matsunaga, T.; Hayashi, T. *Electrochim. Acta* **1981**, *26*, 631.
[16] Harrington, D.A.; Conway, B.E. *Electrochim. Acta* **1987**, *32*, 1703.
[17] Keddam, M.; Rakotomavo, C.; Takenouti, H. *J. Appl.Electrochem*. **1984**, *14*, 437.

[18] Cachet, C.; Wiart, R. *J. Electroanal. Chem*. **1985**, *195*, 21.
[19] Kreiser, H.; Beccu, K.D.; Gutjahr, M.A. *Electrochim. Acta* **1976**, *21*, 539.
[20] Fournier, J.; Brossard, L.; Tilquin, J.Y.; Coté, R.; Dodelet, J.P.; Guay, D.; Ménard, H. *J. Electrochem. Soc.* **1996**, *143*, 919.
[21] De Levie, R. *Adv. in Electrochemistry and Electrochem. Eng.* **1967**, *6*, 329.
[22] Boukamp, B.A. *Equivalent Circuit Users Manual*, University of Twente, **1989**.
[23] Boukamp, B.A. *Solid State Ionics* **1986**, *18-19*, 136.
[24] Boukamp, B.A. *Solid State Ionics* **1986**, *20*, 31.
[25] Macdonald, J.R. *Impedance Spectroscopy*, John Wiley and Sons, **1987**.
[26] Theoridoridou, E.; Jannakoudakis, A.D.; Jannakoudakis, P.D.; Antoniadou, S.; Besenhard, J.O. *J. App. Electrochem*. **1992**, *22*, 733.